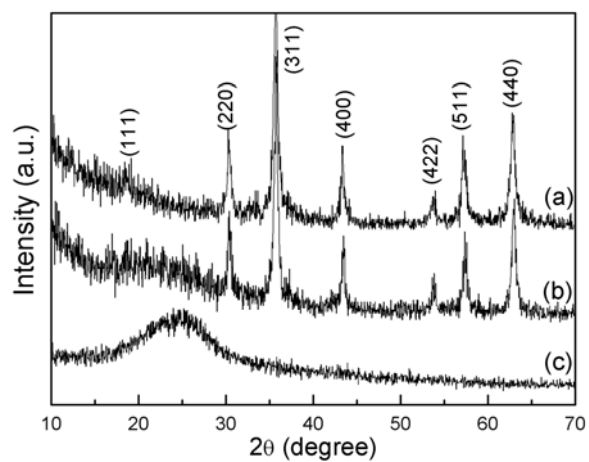
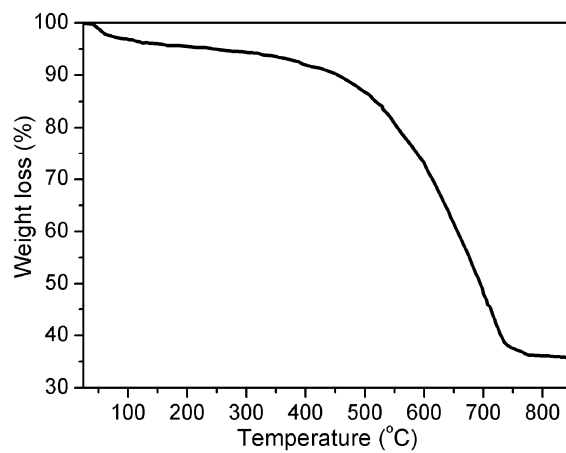


Supporting information:



5 **Fig. S1** XRD patterns of (a) Fe<sub>3</sub>O<sub>4</sub> microspheres, (b) Fe<sub>3</sub>O<sub>4</sub>/PPy composite microspheres and (c) porous PPy microspheres.



15 **Fig. S2** TG analysis of Fe<sub>3</sub>O<sub>4</sub>/PPy composite microspheres.

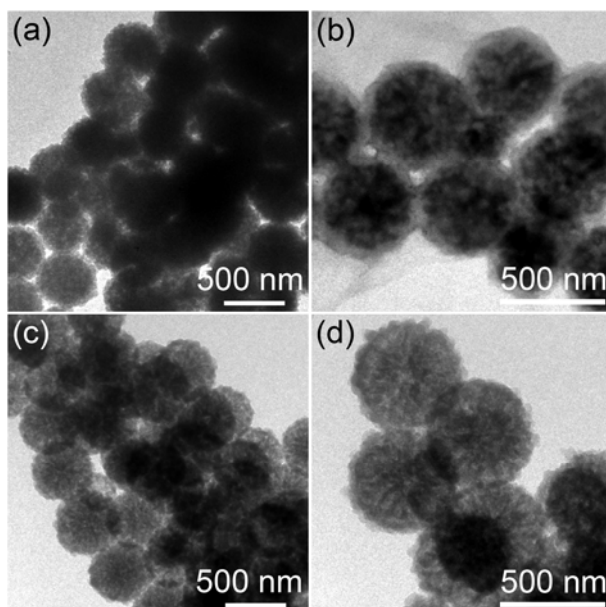


**Fig. S3** TEM images (a) and (b)  $\text{Fe}_3\text{O}_4/\text{PPy}$  composite microspheres synthesized under mechanical stirring for 1.5 h and (c) and (d) their corresponding porous PPy microspheres after residual  $\text{Fe}_3\text{O}_4$  nanoparticles were removed.

5

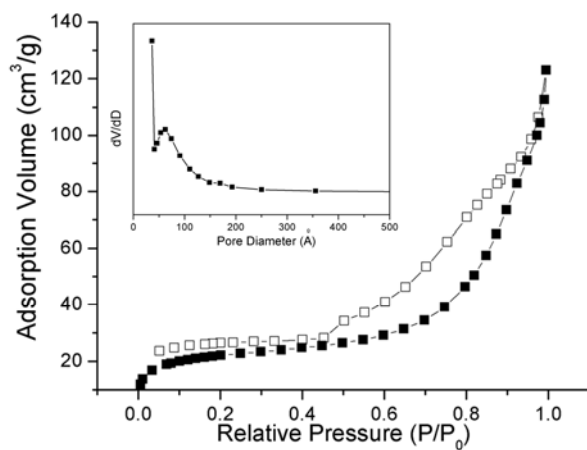


**Fig. S4**  $\text{N}_2$  adsorption/desorption isotherm for the  $\text{Fe}_3\text{O}_4/\text{PPy}$  composite microspheres. (Inset: BJH pore-size distribution curve obtained from the desorption data)

10

**Table S1** Langmuir and Freundlich isothermal parameters for Cr(VI) adsorption on  $\text{Fe}_3\text{O}_4/\text{PPy}$  composite microspheres.

Langmuir			Freundlich		
$Q_m$ ( $\text{mg g}^{-1}$ )	$b$ ( $\text{L mg}^{-1}$ )	$R^2$	$k$	$1/n$	$R^2$
209.2	0.11	0.99	27.97	0.498	0.96

15

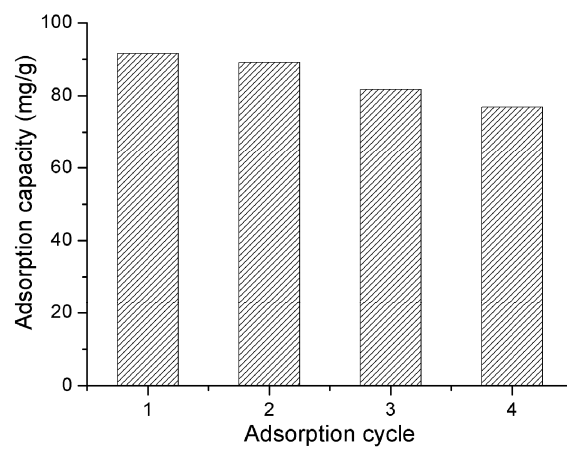


**Fig. S5** Adsorption-desorption cycles.